

## High reflectivity electrofluidic pixels with zero-power grayscale operation

S. Yang, K. Zhou, E. Kreit, and J. Heikenfeld

Citation: [Applied Physics Letters](#) **97**, 143501 (2010); doi: 10.1063/1.3494552

View online: <http://dx.doi.org/10.1063/1.3494552>

View Table of Contents: <http://scitation.aip.org/content/aip/journal/apl/97/14?ver=pdfcov>

Published by the [AIP Publishing](#)

---



## Re-register for Table of Content Alerts

Create a profile.



Sign up today!



# High reflectivity electrofluidic pixels with zero-power grayscale operation

S. Yang,<sup>1</sup> K. Zhou,<sup>2</sup> E. Kreit,<sup>1</sup> and J. Heikenfeld<sup>1,a)</sup>

<sup>1</sup>Novel Devices Laboratory, School of Electronics and Computing Systems, University of Cincinnati, Cincinnati, Ohio 45221, USA

<sup>2</sup>Gamma Dynamics, Cincinnati, Ohio 45221, USA

(Received 19 May 2010; accepted 16 July 2010; published online 4 October 2010)

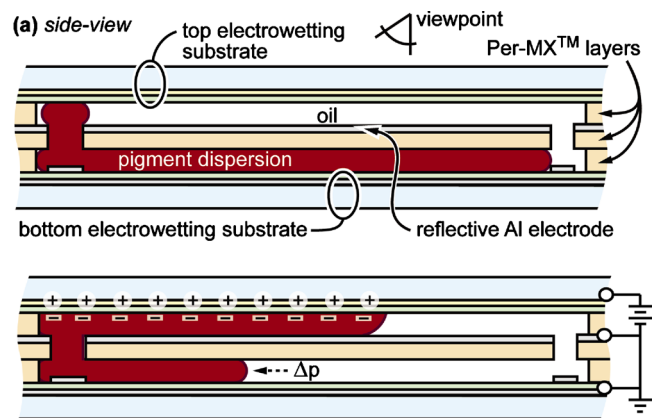
Electrofluidic display pixels are demonstrated with zero-power grayscale operation for 3 months and with  $>70\%$  reflectance. The color of the pixel is changed as electrowetting moves the pigment dispersion between a top and bottom channel. When voltage is removed, a near zero Laplace pressure and a hysteresis pressure of  $0.11 \text{ kN/m}^2$  stabilizes the position. For  $450 \mu\text{m}$  pixels, an electromechanical pressure of  $1.4 \text{ kN/m}^2$  moves the pigment dispersion at a speed of  $\sim 2650 \mu\text{m/s}$ . The predicted switching speed for  $\sim 150 \mu\text{m}$  pixels is consistent with video rate operation (20 ms). The geometrically sophisticated pixel structure is fabricated with only simple photolithography and wet chemical processing. © 2010 American Institute of Physics.

[doi:10.1063/1.3494552]

Electronic paper (e-paper) is now a commercial reality, mainly due to advances in electrophoretic technology.<sup>1</sup> Most e-paper products are currently monochrome with  $\sim 40\%$  white state reflectance. Significant work remains provide full color e-paper that is comparable in brightness to conventional printed media. In addition to bright color, it is highly desirable to implement pixels that retain their image even without electrical power (grayscale-stable). Grayscale-stable operation is also beneficial in terms of display longevity: a grayscale-stable display that switches in 30 ms, and is updated once every 60 s, is only operating for a total of 50 h during 100 000 h of continuous use. A relatively newer e-paper technology, electrowetting (EW) displays<sup>2</sup> have now demonstrated video and  $\sim 20\text{--}30\%$  full color reflectance but require constant electrical power for grayscale operation. A variation in EW displays, termed “droplet-driven” displays<sup>3</sup> has shown bistable and bright monochrome operation but the pixels are very large and only two grayscale states have been shown. Recently, yet another EW variant, the electrofluidic display (EFD), was reported<sup>4</sup> to provide video speed, high pixel resolution, and the potential for bright color due to the use of pigment dispersions similar to those found in inkjet printing. However, like EW displays, constant electrical power is required to hold an image. Reported herein is the first of two methods now in development for creating EFDs that can hold a grayscale image without any electrical power. Also detailed with this report, is a simple fabrication technique for creating geometrically sophisticated fluidic pixels, which may be of broader value to other display and microfluidics researchers.

The grayscale-stable EFD pixel construction is illustrated in Fig. 1(a).  $1 \times 1''$  test pixel arrays were fabricated as follows. A polymer film (Parylene or SU-8) was deposited onto  $\text{In}_2\text{O}_3:\text{SnO}_2$  coated glass to make a bottom EW substrate.<sup>5</sup> SU-8 is particularly useful because it acts as a dielectric and it also promotes adhesion of the next polymer layers. Onto the bottom EW substrate, a DuPont PerMX (Ref. 6) dry film photoresist ( $20 \mu\text{m}$ ) was hot-roll laminated ( $85^\circ\text{C}$ , 40 psi, 1 fpm), photolithographically exposed, and

developed to form a bottom grid of  $450 \times 150 \mu\text{m}^2$  cells with  $30 \mu\text{m}$  grid width. Next, a middle PerMX film was then laminated onto the bottom grids and patterned with  $130 \times 60 \mu\text{m}^2$  and  $130 \times 20 \mu\text{m}^2$  vias at the ends of the pixel cell. Al was vacuum deposited onto the middle PerMX layer, serving as an optical reflector and a ground electrode. The vias through the middle PerMX layer form an overhang, so no patterning of the Al was required to electrically sepa-



(b) top-view photographs of several stable grayscale states

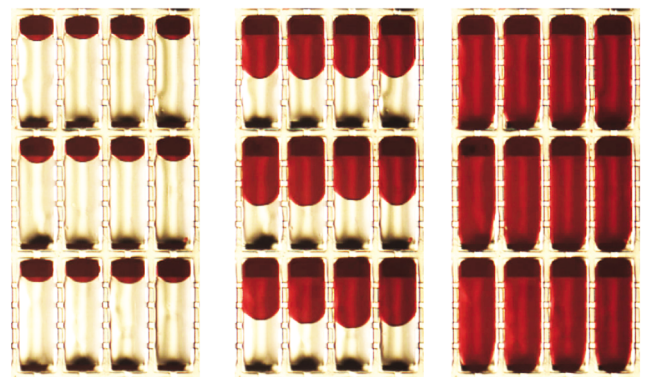


FIG. 1. (Color online) (a) Schematic of grayscale-stable EFD pixel structure and operation. (b) Photographs of three configurations for the pixel: maximum reflection, intermediate grayscale, and minimum reflection.

<sup>a)</sup>Electronic mail: jason.c.heikenfeld@uc.edu.

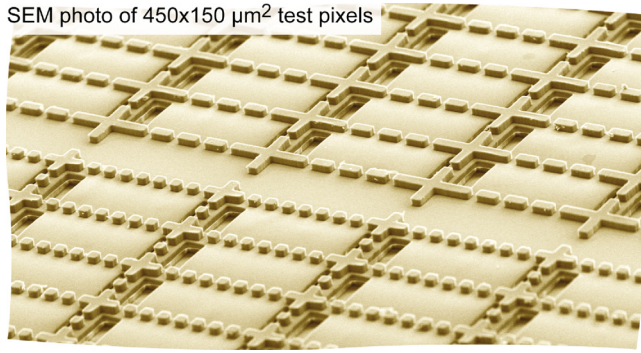


FIG. 2. (Color online) SEM photograph of grayscale-stable EFD test pixels without the fluids or top substrate.

rate Al on the middle PerMX and bottom substrate surfaces. A top PerMX layer was then added in a grid geometry similar to the bottom PerMX. However, as shown in the scanning electron microscopy (SEM) photograph of Fig. 2, the top PerMX grid was discontinuous, to allow self-assembled dosing<sup>4</sup> of pigment dispersion and oil liquids. Before liquid dosing, all featured carried by the bottom substrate were conformally dip-coated with Cytonix Fluoropol 1601 V fluoropolymer. After fluoropolymer coating and self-assembled liquid dosing, the device was sealed with a transparent top EW plate similar to that used in conventional EFDs.<sup>4</sup>

Grayscale-stable EFD pixel operation involves a competition between Laplace pressure, hysteresis, and electromechanical<sup>7</sup> pressure. All surfaces of the completed pixels are uniformly hydrophobic. Therefore, Young's angle for the pigment dispersion in oil is  $\sim 180^\circ$  and the vertical radius of meniscus curvature in the top ( $R_T$ ) and bottom channels ( $R_B$ ) is half of the  $20\ \mu\text{m}$  channel height ( $\sim h/2$ , Fig. 3). Because  $h$  is much smaller than the channel width, the Laplace pressure with no voltage ( $\Delta p_0$ ) can therefore be approximated as  $\Delta p_0 \cong 2\gamma_{ci}/h$  (N/m<sup>2</sup>), where  $\gamma_{ci}$  is the interfacial surface tension N/m between the electrically conducting pigment dispersion and the electrically insulating oil. The top and bottom channel heights are nearly identical, and therefore the Laplace pressure for the pigment dispersion does not change with fluid position. Also, contact angle hysteresis induces a threshold pressure that along with neutral Laplace pressure, stabilizes the positions of the fluids [Fig. 3(a)].

To move the pigment dispersion, a voltage is applied to either the top or the bottom EW substrates. As illustrated in

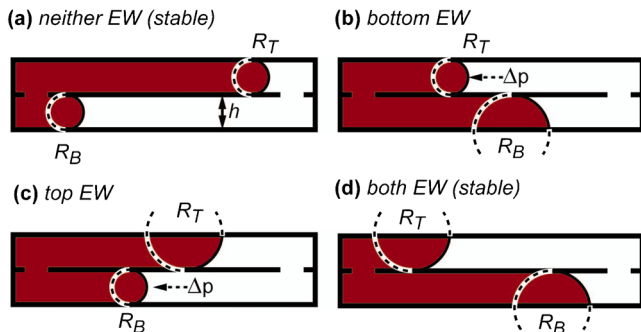


FIG. 3. (Color online) EW induced pressure difference actuates the pigment movement. Illustrated states are: (a) stable when neither channel is electrowetted; (b) pigment moving to the bottom; (c) pigment moving to the top; and (d) stable when both channels are electrowetted.

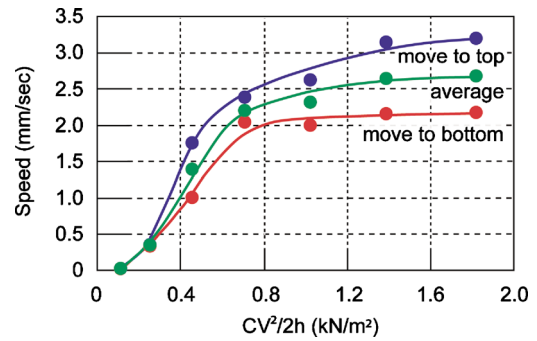


FIG. 4. (Color online) Pixel switching speeds vs applied electromechanical pressure.

Fig. 3, EW (Ref. 5) causes the contact angle to reduce from Young's angle  $\theta_Y$  to the electrowetted contact angle  $\theta_V$  according to the EW equation:  $\cos \theta_V = (\gamma_{id} - \gamma_{cd}) / \gamma_{ci} + CV^2 / 2\gamma_{ci}$ , where  $C$  is the capacitance per unit area of the EW dielectric,  $\gamma$  is the interfacial tension between the conducting pigment dispersion ( $c$ ), insulating oil ( $i$ ) and the dielectric ( $d$ ), and  $V$  is the applied dc or ac rms voltage. The contact angle reduction results in an increase in  $R_T$  or  $R_B$  according to  $R = -h / (\cos \theta_V + \cos \theta_Y)$ . Therefore, the pressure with voltage acting on the pigment dispersion in the top or bottom channel can be simplified to

$$\Delta p_V = (2\gamma_{ci} - CV^2/2)/h. \quad (1)$$

Now, as illustrated in Figs. 3(b) and 3(c), an imbalanced pressure between the top and bottom channel can cause the pigment dispersion to move to the channel with lower pressure (greater  $V$ , larger  $R$ ). Applying equivalent voltages on both substrates, or removing all voltages, would stabilize the pigment dispersion (stop movement), as illustrated in Figs. 3(d) and 3(a), respectively. Demonstration of stable positioning of the pigment dispersion in several grayscale positions is shown in the photographs of Fig. 1(b).

Equation (1) is a static model only. During movement of the pigment dispersion, there are two additional pressures that must be considered. First, there is the well-known effect of contact angle hysteresis. As shown in Fig. 4, a threshold pressure of  $\sim 0.11\ \text{kN/m}^2$  is required to begin to move the pigment dispersion. To achieve this threshold pressure, voltages for tested dielectrics include  $\sim 25\ \text{V}$  for  $\sim 5\ \mu\text{m}$  SU-8 ( $\epsilon_r = 3.2$ ),  $\sim 8.4\ \text{V}$  for 300 nm of Parylene HT (Ref. 8) ( $\epsilon_r = 2.2$ ), and  $\sim 3.3\ \text{V}$  for 150 nm of  $\text{Si}_3\text{N}_4$  ( $\epsilon_r = 7$ ). If this threshold is dominated by contact angle hysteresis, then there is  $\sim 7^\circ$  of hysteresis due to dielectric roughness, dielectric charge injection, and/or other pixel imperfections. This hysteresis pressure reduces the driving pressure, and slows device switching speed. However, some level of hysteresis pressure is absolutely essential for stable positioning of the pigment dispersion, because the top and bottom channel heights can never be perfectly equal.

During movement of the pigment dispersion, in addition to hysteresis pressure there is another pressure that slows the pixel operating speed. There is a dissipative<sup>9</sup> force per unit length  $f_D$  (Newton per meter), which mainly consists of fluid drag and channel wall shear. This dissipative force results in a dissipative pressure calculated by  $f_D/h$ . The dissipative pressure only increases as the speed of fluid movement is increased. As seen in Fig. 4, the speed of fluid movement begins to saturate at  $\sim 1\ \text{kN/m}^2$ . This saturation of switch-

ing speed most likely corresponds to the onset of contact angle saturation<sup>5</sup> and/or increasing influence of the dissipative pressure.

Measured using a high speed camera, the maximum average switching speed is  $\sim 2650 \mu\text{m/s}$ . For the 450  $\mu\text{m}$  long pixel, this speed results in  $\sim 170$  ms switching time ( $\sim 6$  Hz refresh rate). By scaling down the pixel length by one-third to  $\sim 150 \mu\text{m}$  (170 dpi), this refresh rate can be increased by  $9\times$  ( $\sim 20$  ms, 50 Hz) as the distance the fluids move is decreased by  $3\times$  and the drag force is reduced by  $3\times$ . This prediction is based on the  $d/L$  scaling factor proven for EW lab-on-chip devices<sup>9</sup> when  $d/L$  is sufficiently small<sup>10</sup> ( $d/L = 0.044$  for the pixels reported herein). Fluid viscosities and interfacial surface tensions are unoptimized for the devices reported herein. Therefore device scaling and optimized materials should easily satisfy video speed requirements. Also observed in Fig. 4, the speed to move pigment dispersion from the bottom channel to the top channel is faster than the opposite movement. This indicates that the upper channel has a greater height due to possible compression of the bottom PerMX layer after the multilamination fabrication process, or due to a top substrate that is not fully compressed against the top PerMX layer.

The stability of position of the pigment dispersion was tested for 3 months, and no movement was observed for any orientation of the test module. This demonstrates true or “infinite” bistable operation, because the pixels will not change until suitable voltage applied. Furthermore, no holding capacitor or other stored charge is required to sustain the pixel in a grayscale state. Also, a variety of different grayscale states were demonstrated. The number of accessible grayscale states is limited only by the quality of reproduction of the pixel structures and the resolution of the voltage controls. Time modulated grayscale level selection and/or voltage level control could be used and should allow grayscale operation adequate for e-paper applications. In addition, the basis for intermediate grayscale reset states has been demonstrated and will be presented in a future report.

The bistable EFD pixels exhibit a bright reflectance. Unlike a conventional EFD device, the pigment dispersion can be hidden in the bottom channel, and the optical loss associated with a fully visible reservoir<sup>4</sup> is reduced. Plotted in Fig. 5 are the maximum and minimum reflections with use of a red pigment dispersion. The measured white state reflectance is as high as 75% in the visible light region. This is comparable to the reflectance of conventional white paper. Currently, the dark state reflectance is  $\sim 25\%$ , resulting in a limited contrast ratio. The contrast ratio can be substantially improved by implementation of antireflection coatings on the front glass, with use of index-matched  $\text{In}_2\text{O}_3:\text{SnO}_2$ , by using a black colored material in place of the top PerMX layer, or by patterning the Al reflector such that it does not create reflective area in the interpixel space. Even with these con-

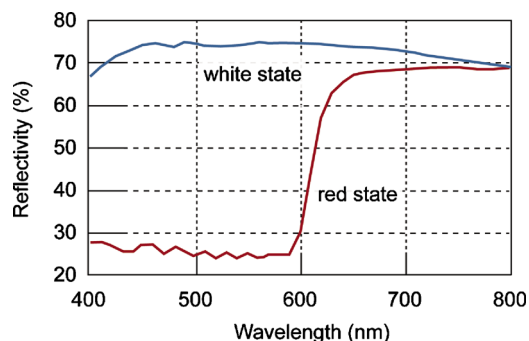


FIG. 5. (Color online) Measured reflectivity for an array of grayscale-stable EFD pixels in the white and red reflective states.

trast enhancing improvements, the theoretical white state reflectance can be very high. Assuming vias in the middle PerMX layer of 12% area, 90% reflective Al, 5% loss for a black pixel border, and 3% loss at the front transparent electrode, a reflectivity of 72% is predicted. Due to light out-coupling, some additional light loss can also occur when using black oil and a white scattering pigment dispersion. This bright white reflection, zero-power grayscale operation, fast switching speed, and simple fabrication make EFDs potentially attractive for the next generation of e-paper technology.

The authors acknowledge partial support from NSF Career Award No. 0640964 (University of Cincinnati), NSF SBIR No. 0944455 (Gamma Dynamics), an ARL Grant No. W9111NF-09-2-0034 (Dave Morton and Eric Forsythe), and AFRL Contract No. 5408-25-SC-0003 (Rajesh Naik). The authors would like to thank Chester Balut and Yun Hao (DuPont), Ken Dean, Steve Smith, Brian Broliier, and John Rudolph (Gamma Dynamics) and Russ Schwartz, Jack Gormely, Lisa Clapp, April Milarcik, Stan Vilner (Sun Chemical) for their materials/technical support and encouragement on this work.

<sup>1</sup>B. Comiskey, J. D. Albert, H. Yoshizawa, and J. Jacobson, *Nature (London)* **394**, 253 (1998).

<sup>2</sup>R. A. Hayes and B. J. Feenstra, *Nature (London)* **425**, 383 (2003).

<sup>3</sup>K. Blankenbach, A. Schmoll, A. Bitman, F. Bartels, and D. Jerosch, *J. Soc. Inf. Disp.* **16**, 237 (2008).

<sup>4</sup>J. Heikenfeld, K. Zhou, E. Kreit, B. Raj, S. Yang, B. Sun, A. Milarcik, L. Clapp, and R. Schwartz, *Nat. Photonics* **3**, 292 (2009).

<sup>5</sup>F. Mugele and J.-C. Baret, *J. Phys.: Condens. Matter* **17**, R705 (2005).

<sup>6</sup>DuPont PerMX data sheet: <http://www.microresist.de/produkte/dupont/pdf/permxseries.pdf>.

<sup>7</sup>T. B. Jones, *J. Micromech. Microeng.* **15**, 1184 (2005).

<sup>8</sup>M. Dhindsa, S. Kuiper, R. Kumar, and J. Heikenfeld, “Reliable and low-voltage electrowetting on thin parylene films,” (unpublished).

<sup>9</sup>J. H. Song, R. Evans, Y.-Y. Lin, B.-N. Hsu, and R. B. Fair, *Microfluid. Nanofluid.* **7**, 1613 (2009).

<sup>10</sup>R.-F. Yue, J.-G. Wu, X.-F. Zeng, M. Kang, and L.-T. Liu, *Chin. Phys. Lett.* **23**, 3313 (2006).